APPLICATIONS OF NEUTRON SCATTERING TO PROBLEMS IN MATERIALS SCIENCE

J. R. WEERTMAN*
* Northwestern University, Dept. of Materials Science and Engineering and the Materials Research Center, Evanston, IL 60201

ABSTRACT

Neutrons possess a number of attributes which make neutron scattering a powerful technique for the investigation of problems in materials science. These properties are discussed with emphasis on their importance to materials characterization. A number of recent experiments using neutron scattering will be described. These studies include the areas of damage accumulation; residual stress; porosity in ceramics; polymer chain configurations; phase changes.

INTRODUCTION

The technique of thermal neutron scattering has proved to be of extraordinary value in the characterization of materials. In many cases the detailed information provided by the scattered neutrons can be obtained by no other method. The formal theory of neutron scattering is similar in many respects to that for x-rays. However neutrons possess a number of special properties which make them exceptionally useful in materials research. Perhaps the most striking feature of neutrons is their great penetration depth. Specimens used in neutron scattering experiments typically are several millimeters thick so that volumes of the order of a cubic centimeter are irradiated. Therefore truly bulk properties are measured, largely undistorted by the presence of a surface. It becomes possible to study phenomena which of necessity require the survey of many grains (such as grain boundary cavitation or bulk microcracking) or objects which are themselves comparable to, or larger than the penetration depth of x-rays (e.g., pores in ceramics). The large penetration depth permits the study of stress states and of texture as a function of position in a component.

Another important property of neutrons is the form of the dependence of scattering length on atomic number. Unlike the case of x-rays neutron scattering lengths are not a monotonic function of atomic number but rather show a more random behavior. The precipitation kinetics of alloys which contain elements situated close to one another in the periodic table frequently can be followed easily by neutron scattering whereas with x-rays the scattering contrast between constituents is too small to make an experiment feasible. A fortunate circumstance is the fact that several light elements, most notably hydrogen and deuterium, are comparatively good neutron scatterers. Happily hydrogen and deuterium differ considerably in their scattering lengths. The technique of selective deuteration has been used with great success to study polymer and micelle configurations. In this fashion long standing disputes about the morphology of polymer chains have been settled.

Neutrons interact with the nuclei of atoms. Hence in structural determinations neutron scattering gives information directly as to positions of the nuclei in the crystal whereas with x-rays this information is convoluted with the electron positions. In the case of magnetic materials there is an additional contribution to the scattering arising from the interaction of the magnetic moments of the neutrons with those of the atoms. Neutron scattering has been, and continues to be of incalculable value in the elucidation of magnetic structures.

A number of books and review articles (e.g., [1-4]) treat the mathe-

Mat. Res. Soc. Symp. Proc. Vol. 41. © 1985 Materials Research Society

matical formalism of neutron scattering, discuss the type of information that can be extracted from scattering patterns, and describe experimental details of the measurements. In the following sections brief descriptions are given of a number of recent experiments which illustrate the use of neutron scattering techniques to characterize materials.

STUDIES OF DAMAGE ACCUMULATION

Bulk microcracking in a ceramic

Small angle neutron scattering (SANS) has been used by Case and Glinka [5] to study the extent and character of bulk microcracking in the ceramic $YCrO_3$. This material undergoes a phase transformation at 1100°C. Microcracking is produced as the material cools through the transformation temperature after it has been sintered. Prolonged annealing below 1100°C heals the cracks whereas reheating above this temperature returns the material to its initial microcracked state. Since the material initially was sintered around 1750°C the subsequent heat treatments at the much lower temperature of 1100°C leave the microstructure essentially unchanged except for the introduction or healing of the microcracks. Material with this behavior is ideally suited for SANS measurements: subtraction of the scattering of a specimen in the healed state from the scattering when it is cracked eliminates the contributions from all other sources, such as the surfaces. Since it was suspected that, at least in two dimensions, the cracks are quite large (several micrometers in extent), it was necessary to establish whether the scattering is controlled primarily by the principles of diffraction or if refraction effects have become important. In the former case the differential scattering cross section $d\Sigma/d\Omega$ depends on neutron wave length λ only through the scattering vector $\underline{Q}$. (The magnitude of the vector $\underline{Q}$ is equal to $4\pi \sin\theta/\lambda$, where 2θ is the scattering angle.) When the scattering entities become so large that refraction begins to be appreciable, curves of $d\Sigma/d\Omega$ vs Q are no longer independent of λ. Tests carried out at several wave lengths showed that the scattering from the microcracks in $YCrO_3$ is indeed diffractive. The data can be fit to the curve of scattering expected from an ensemble of randomly oriented thin disks of height 2H and radius 2a (Fig. 1). An average height of 24 nm was obtained from the curve fitting procedure. Elasticity measurements in conjunction with the scattering data yielded values for the average crack radius and crack density. The average crack radius, 5.7 μm, has the expected value of 1 - 2 grain diameters.

The results of the $YCrO_3$ experiment demonstrate that SANS can be used to detect the onset of microcracking in brittle materials as well as to quantify the extent of damage. It is possible that microcracking in metals (including grain boundary cracking) also can be studied by SANS.

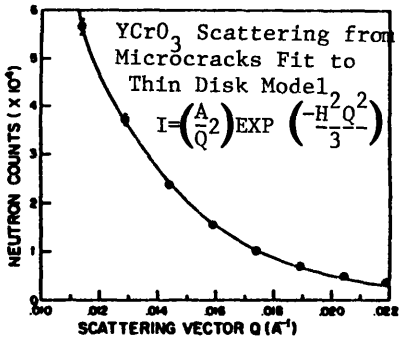

FIG. 1. Scattering intensity vs scattering vector for $YCrO_3$ containing microcracks. The curve is a least-squares fit to the data of the scattering function for randomly oriented thin disks of thickness 2H = 24 nm [5].

https://doi.org/10.1557/PROC-41-73 Published online by Cambridge University Press

Radiation damage

Radiation damage frequently appears in the form of voids. (The use of SANS to study cavitation will be treated in a subsequent section.) Another form of radiation damage occurs in precipitation-hardening steel containing a small percentage of copper. This material becomes embrittled after exposure to neutron irradiation. It was suspected that the embrittling agents are either small voids or copper-rich clusters produced by the radiation, but the features are too small to be detected with clarity in a ferromagnetic material by transmission electron microscopy. This problem has been studied by SANS [6] and further work is in progress [7].

Since iron is ferromagnetic the neutrons in a SANS experiment are scattered not only by heterogeneities in the composition of the specimen but also by its magnetic domains. To eliminate the complication of superimposed refraction from domains the specimen usually is magnetized in the plane perpendicular to the neutron beam. In the expression for the differential scattering cross section for such a magnetized ferromagnetic specimen the factor $(\Delta\rho_{nuc})^2$ is replaced by $[(\Delta\rho_{nuc})^2 + \sin^2\alpha\ (\Delta\rho_{mag})^2]$. Here $\Delta\rho_{nuc}$ and $\Delta\rho_{mag}$ are the differences in nuclear and magnetic scattering length density between matrix and scattering entity and α is the angle between the imposed magnetic field $\underline{H}$ and the scattering vector $\underline{Q}$. The ratio of $d\Sigma/d\Omega$ measured perpendicular to $\underline{H}$ to its value parallel to the field gives directly the quantity $[(\Delta\rho_{nuc})^2 + (\Delta\rho_{mag})^2]/(\Delta\rho_{nuc})^2 = A$. Frisius, Kampmann, Beaven and Wagner [6] compared measured values of A with calculations based on scattering arising from Cu precipitates in iron (A = 11.1) and from voids (A = 1.3). For iron containing small amounts of copper A was found to equal 11.1, indicating that the scattering is caused by copper precipitates. Size distribution curves derived from the SANS data gave a value of 2.2 nm for the radius of the precipitates induced by fast neutron irradiation. Odette and Glinka [7] are studying the effects of neutron irradiation (total fluence of $10^{23}/m^2$ at ~290°C) on a plain carbon steel containing 0.35 wt.% Cu. Figure 2 shows plots of scattering intensity vs Q for a magnetized irradiated specimen. It can be seen that there is an appreciable difference between the scattering intensities perpendicular and parallel to the magnetic field. The ratio of the scattering in the two directions is greatest at $Q \sim 0.7\ nm^{-1}$ and serves to identify the source of scattering as particles which are roughly 50/50 Cu-Fe. The average diameter of these particles is about 4 nm and their number density is $2 - 5 \times 10^{22}/m^3$. At higher values of Q the ratio of the scattering intensity in the two directions drops to a level consistent with scattering from voids. Thus the SANS measurements show that (in agreement with Frisius et al. [6]) the irradiated samples contain copper-rich particles and even smaller voids or vacancy clusters. The small defects may enhance diffusion and thus promote formation of the precipitates. These experiments nicely illustrate the fact that, in the case of magnetic materials, additional information is provided by the magnetic component of $d\Sigma/d\Omega$.

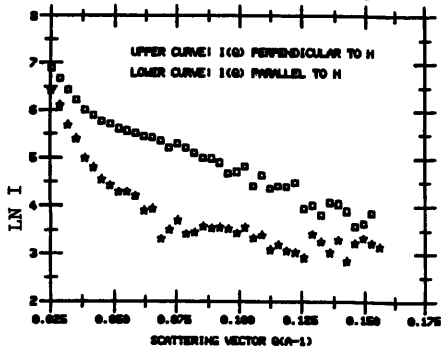

FIG. 2. Curves showing the dependence of scattered intensities parallel (stars) and perpendicular (squares) to an imposed magnetic field. Irradiated Fe-C containing 0.35 wt.% Cu [7].

https://doi.org/10.1557/PROC-41-73 Published online by Cambridge University Press

Microstructural changes produced by high temperature service

Several SANS studies (e.g., [8,9]) have been carried out of the effect of high temperature service on the size of γ' particles in a nickel base superalloy. Since the strength of an alloy containing dispersed particles depends on their size and distribution, any coarsening is likely to result in a degradation of the material's mechanical properties. Recently the effects of high temperature exposure, with and without deformation, have been investigated in a ferritic stainless steel, Fe9Cr1Mo modified with the addition of small amounts of the strong carbide formers V and Nb [10]. This steel is a candidate material for use in power generation applications, where it must maintain its ability to withstand static and cyclic loading even after prolonged periods at elevated temperatures. The modified Fe9Cr1Mo is used in the fully tempered martensitic state. Its initial microstructure may be characterized as a lath structure with a high dislocation density and containing a dispersion of fine $V_xNb_{1-x}C$ carbides. Degradation of the material's strength is associated with the formation of equiaxed subgrains, a clearing out of the dislocations and coarsening of the MC carbides and growth of chromium-rich $M_{23}C_6$ carbides. Experiments have been carried out to see if these microstructural changes can be followed by SANS. In one series of SANS measurements, the effect of aging temperature on the carbide population in modified Fe9Cr1Mo aged isothermally for 5000 h was investigated. The size distributions of the carbides deduced from the scattering curves are shown in Fig. 3. It can be seen that aging at 538°C produces the highest density of fine carbides. Shifting to higher aging temperatures results in coarsening and a drastic decrease in the carbide density. These results are consistent both with TEM observation [11] and with measurements of the hardness as a function of aging temperature (Fig. 4). Similar correlations have been made between the pronounced cyclic softening observed in the steel at elevated temperatures and changes in the carbide population as deduced from SANS measurements. It is rather surprising that the SANS-derived size profiles, calculated with an average scattering length density for the carbides, agree so well with the TEM and hardness results. The composition, and thus the scattering length densities of the carbides are changing continuously during time at high temperature. This situation points up one of the problems associated with SANS measurements in complex materials. It is difficult, if not impossible, to separate the scattering components arising from several classes of scattering entities when each of these entities changes from one specimen to another in a series of tests.

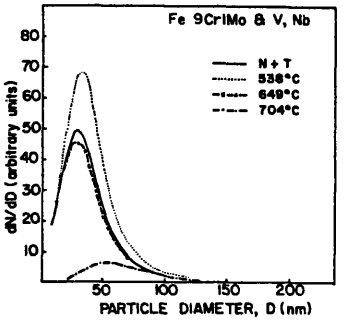

FIG. 3. Size distributions dN/dD of the carbides in modified Fe9Cr1Mo aged 5000 h at 538°, 649°, or 704°C, or normalized and tempered only [10].

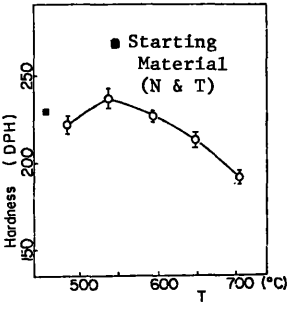

FIG. 4. Hardness as a function of aging temperature. Modified Fe9Cr1Mo aged 5000 h [10].

https://doi.org/10.1557/PROC-41-73 Published online by Cambridge University Press

Grain boundary cavitation

Grain boundary cavitation is an important damage mechanism at high temperatures. A large number of metals and alloys, when subjected to deformation at elevated temperatures, develop small voids on their grain boundaries. These voids grow under continued deformation and eventually may coalesce, thereby causing failure. Cavitation is an important engineering problem but it also is of considerable scientific interest. How do voids nucleate? Why do they grow under certain conditions? A great deal of effort has been expended on the theory of cavitation but almost no data exist of the type which would permit the testing of the theories. The sort of information needed includes the number densities of the voids and their size distributions as functions of time, temperature and deformation parameters. For reliable results a large number of voids should be included in the sample. In typical SANS specimens some 10^{6} - 10^{12} voids are included in each measurement. The voids nucleate only at grain boundaries, so their total volume fraction is quite small. It is possible with SANS to measure void volume fractions which are as small as 10^{-6}. Observations of voids should begin as close as possible to the nucleation event, but since nuclea-

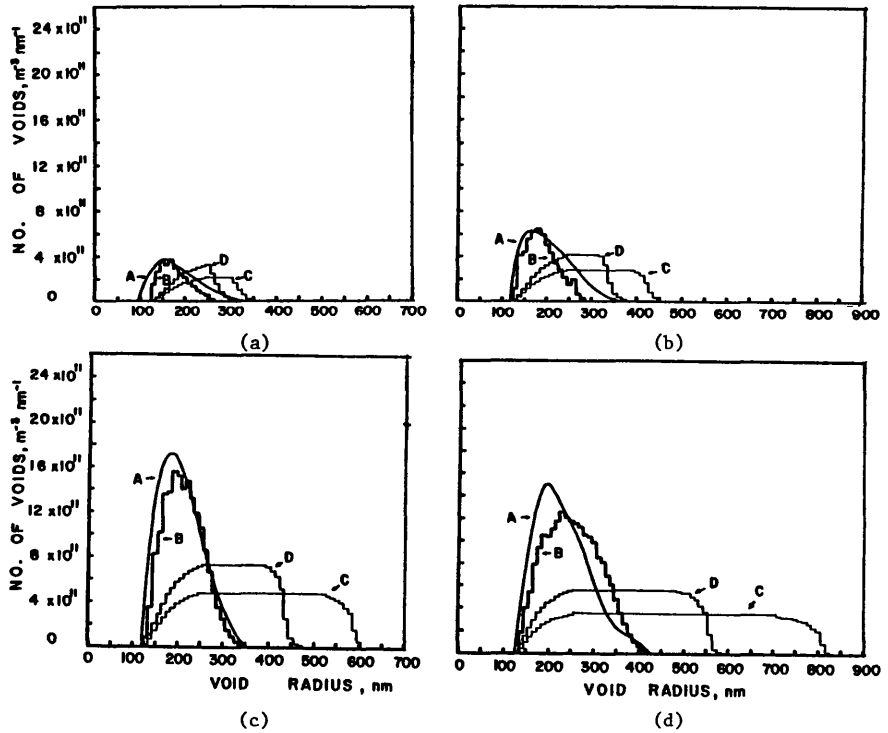

FIG. 5. Void size distribution curves for Cu crept at 405°C under a stress of 27.6 MPa for (a) 1.1 x 10^{4} s, (b) 2.2 x 10^{4} s, (c) 4.3 x 10^{4} s, (d) 7.7 x 10^{4} s. Smooth curves (A) are obtained from the SANS measurements. The other curves are calculated on the basis of void growth models based on grain boundary vacancy diffusion (B), and diffusion coupled with matrix plasticity with (D) and without (C) surface energy forces taken into account [13].

https://doi.org/10.1557/PROC-41-73 Published online by Cambridge University Press

tion is continuous it also is necessary to be able to include large voids. Void sizes in the range of a few nanometers to somewhat less than a micrometer can be detected by SANS and analysed by diffraction theory. Of great importance, it is possible with SANS to separate void nucleation from void growth so that these two phenomena can be distinguished.

An extensive study of grain boundary cavitation in a model system, high purity copper, has been carried out with SANS [12-16]. The size distributions of voids in copper crept at 405°C (1/2 the absolute melting temperature) under a stress of 27.6 MPa for varying amounts of time are shown in Fig. 5 (curves A). The detailed information provided by the SANS measurements (e.g., nucleation rates, average void spacings) permits calculation of the size distribution curves predicted by various growth theories (curves B, C, D). Thus, for the first time, it is possible to make a quantitative evaluation of the merits of the various cavitation models. The information obtained from the SANS measurements is quite unique and should prove to be of great value in the investigation of cavitation processes.

Ceramics as well as metals cavitate and the methods described above have been used to study the phenomenon in a number of ceramic materials [17-19].

RESIDUAL STRESS AND TEXTURE MEASUREMENTS

Another application of neutron scattering to materials research which has considerable scientific and technological potential is the measurement of residual stresses. Because of the large penetration depth of neutrons it is possible to use a slit system to measure stress as a function of position. Thus stress states can be determined through the thickness of a component without destroying it. The validity of the method has been verified by experiments on test bars in which the stress state is known [20, 21].

One investigation [22, 23], the measurement of stresses in cermets, will serve to illustrate the use of neutrons in the study of residual stresses. These experiments were carried out at the Intense Pulsed Neutron Source at Argonne National Laboratory. Cermets are very hard materials consisting of small pieces of a hard carbide in a soft binder, in this case tungsten carbide in a cobalt nickel alloy. Because of the large difference in the thermal coefficients of expansion between tungsten carbide and the binder, huge hydrostatic stresses are built up during fabrication of the material: tensile in the binder and compressive in the carbide. In this particular experiment the effect of various forms of applied stress on relaxing the large hydrostatic stresses was investigated. It was found that modest amounts of straining or cycling produce relaxations of the order of GPa's. Such a change in the internal stress state under loading certainly must affect the behavior of the cermets during service. A result which makes the data seem very convincing is the fact that the volume averages of the measured stress changes are zero (to within experimental error), as indeed they should be.

Residual stress measurements by neutrons should be useful in the examination of welds, to study load sharing, the effects of heat treatment, mechanical treatment. Improved instrumentation and increased neutron fluxes will improve the spatial resolution, currently about 1 mm^2.

The ability of neutrons to interrogate large volumes also make them useful in the study of texture development. Recently on-line instrumentation for texture determination has been devised [24] which permits the kinetics of recrystallization to be studied.

POROSITY CHARACTERIZATION

As mentioned in the introduction, the ability of neutrons to penetrate substantial thicknesses of material opens the door to the possibility of investigation by neutron scattering of "large" microstructural features. In

https://doi.org/10.1557/PROC-41-73 Published online by Cambridge University Press

general, the scattering of neutrons with the wave lengths ordinarily used in SANS experiments follows the theory of diffraction if the scattering entities are less than a few tenths of a micrometer. Refraction is dominant in the case of heterogeneities larger than about 10 μm. In the intermediate size range scattering occurs by a mixture of diffraction and refraction. If the density of scatterers is high multiple scattering effects profoundly influence the shape of the scattering curve and its dependence on neutron wave length. The theory of scattering in the intermediate range between pure diffraction and the dominance of refraction, with the added complication of strong multiple scattering effects, is currently being developed [25]. Thus the range of features which may be studied and analysed by neutron scattering is opening up to the point of overlap with other NDE techniques. This new development is proving to be especially valuable in the study of porosity and sintering in ceramics. From measurements of beam broadening as a function of neutron wave length in direct beam experiments it is possible to determine the average radius of the scatterers and their density. Figure 6 shows the dependence on neutron wave length of the radius of curvature r_c at Q = 0 of the circularly averaged scattering curves for the ceramic $YCrO_3$ in three states: powder, green compact and sintered [26]. The points represent experimental data and the lines are theoretical calculations. It can be seen that the agreement between theory and experiment is excellent. Sample thickness and average size and density of the scatterers are parameters which enter into the curve fitting. The scatterers are taken to be the powder particles in the case of $YCrO_3$ powder, to be voids when the material is in the green state or is sintered. The diameters of the scatterers are found to be 0.89, 1.1 and 2.1 μm for the powder, green compact and sintered material, respectively. The development of scattering theory to include the effects of refraction and strong multiple scattering extends the investigation by scattering to such features as large pores in metals and ceramics, and magnetic domains. With increased flux and improved instrumentation it should be possible to follow the process of sintering in real time.

In a quite different type of experiment involving a study of porosity in a ceramic material, SANS has been used to study the size and surface area of pores in silica particles used in liquid chromatography [27]. The accessibility of the pores in the silica particles has been measured by saturating samples with an H_2O/D_2O solution whose neutron scattering length density matches that of silica. Any residual scattering observed under this condition can be attributed to closed (inaccessible) pores. This technique should find application in the characterization by SANS of porous silica supports in metal catalysts.

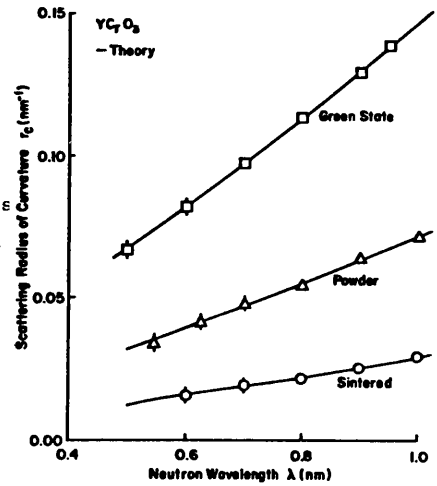

FIG. 6. Radius of curvature r_c at Q = 0 vs neutron wave length λ for circularly averaged scattering curves of $YCrO_3$ in the following conditions: powder, green state, sintered. Points are experimental data. Lines are theoretically derived from the theory of multiple scattering [26].

https://doi.org/10.1557/PROC-41-73 Published online by Cambridge University Press

POLYMERS

The large difference in the scattering lengths b of hydrogen and deuterium has already been mentioned ($b_H = -3.7 \times 10^{-15}$ m vs $b_D = +6.6 \times 10^{-15}$ m). Because of this difference, together with the fact that both hydrogen and deuterium are strong scatterers, it is possible to investigate a large number of problems in polymer configuration by means of neutron scattering. Indeed, neutron scattering has proved to be an excellent, unmatched technique for examining polymeric structures. Typically a fraction of the chains, or segments of chains in a specimen are made with deuterium in place of hydrogen. The deuterated material then is mixed with the ordinary protonated polymer. Measurements by SANS of the radius of gyration of the deuterated chains in such a mixture settled a long standing controversy regarding the molecular conformation in amorphous polymers. Are the chains arranged in random (Gaussian) coils as proposed by Flory and co-workers, or in quasi-parallel bundles? (See [28].) Such experiments have been extended to the intermediate Q range in order to examine the local chain conformation over distances of the order of 1 - 10 nm.

Active areas of research in polymeric structures which are being investigated by neutron scattering include the following: polymer-polymer interactions in blends (compatibility, morphology of second phase, optimization of processing), diffusion of polymers, colloidal systems, micelles, response to deformation (individual chains, crystalline polymers). Interactions in blends of polymers in which one species is deuterated are examined by SANS to determine the compatibility of the constituents. Information on the morphology of two phase blends can be used to optimize processing variables. Diffusion in polymers is being measured by noting changes in scattering as a function of time and temperature from samples prepared by alternating layers of deuterated and protonated polymers [29,30]. As larger neutron fluxes become available it will be of great interest to follow the dynamics of changes in chain configuration during deformation.

PHASE TRANSFORMATIONS

A number of experimenters have taken advantage of the penetrating power of neutrons and of the large variability in scattering length between elements with similar atomic number to study phase transformations by neutron scattering (e.g., [31-33]). An interesting example is provided by a current study of the precipitation of the ω phase in β -III titanium [34,35]. Fatemi and colleagues have shown that when the solution treated and quenched titanium alloy is brought quickly up to the temperature at which β transforms to the β + ω field (i.e., when the transformation takes place isothermally), the small athermal ω precipitates in the as-quenched material align and cluster into long rods oriented along the [111] directions. This orientation preference of the ω phase is manifested in isointensity curves on the 2 dimensional neutron detector with a strong 4-fold symmetry. Upon continued aging the intensity of small angle scattering increases over an extended period of time but the value of Q at which the scattering is a maximum remains constant (see Fig. 7). The peak in the curves of scattered intensity vs Q arises from interparticle interference. Its position gives an indication of the average interparticle spacing. Fatemi [35] interprets this period in which the amount of scattering continues to increase yet the number of particles appears to be constant as a time of "constant size diffusion ripening". During this time the size of the rod-like ω particles remains unchanged but their composition is continually changing via diffusional transport toward the equilibrium value. As the composition changes the scattering contrast between the β and ω phases grows and thus the intensity of scattering scales upward without a shape change. Eventually equilibrium is attained, ordinary coarsening begins and the position of the peak in the scattering curve shifts to lower Q's.

https://doi.org/10.1557/PROC-41-73 Published online by Cambridge University Press

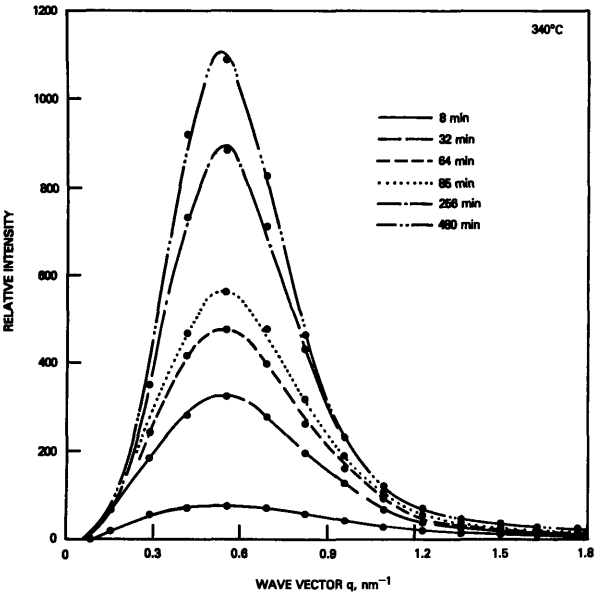

FIG. 7. Intensity profiles produced by the rod-like ω particles in β-III titanium held for various lengths of time at 340°C.

ACKNOWLEDGMENTS

This work was supported by the Department of Energy, Grant DE-AC02-81ER10960, and the National Science Foundation, Grant DMR-8320157. Parts of this paper are based on a workshop presentation "Scientific Opportunities with Neutrons in Materials Science", Major Materials Facilities Committee, Commission on Physical Sciences, Mathematics and Resources, National Research Council, 17 March 1984, Washington, D. C., National Academy Press, 1984.

REFERENCES

1. G. E. Bacon, "Neutron Diffraction," 3rd ed., Oxford University Press, 1975.
2. Treatise on Materials Science and Engineering, Vol. 15, "Neutron Scattering," G. Kostorz, Ed., Academic Press, New York, 1979.
3. C. J. Glinka, H. J. Prask and C. S. Choi, "Mechanics of Nondestructive Testing," W. W. Stinchcomb, Ed., p 143, Plenum Press, New York, 1980.
4. J. R. Weertman, "Nondestructive Evaluation: Microstructural Characterization and Reliability Strategies," O. Buck and S. M. Wolf, Eds., p.147, TMS-AIME, Warrendale, PA, 1981.
5. E. D. Case and C. J. Glinka, J. of Mats. Sci., 19 (1984) 2962.
6. F. Frisius, R. Kampmann, P. A. Beaven and R. Wagner, "Dimensional Stability and Mechanical Behavior of Irradiated Metals and Alloys," British Nuclear Energy Society, London, p 171, 1983.
7. G. R. Odette and C. J. Glinka, to be published.

8. P. Pizzi, H. Walther and P. Cortese, Proc. 8th World Conf. Nondestr. Test., p 3L7, 1976.
9. D. Schwahn, W. Kesternich and H. Schuster, Met. Trans. A 12A (1981) 155.
10. S. Kim, J. R. Weertman, S. Spooner, C. J. Glinka, V. Sikka and W. Jones, "Nondestructive Evaluation: Application to Materials Processing", edited by O. Buck and S. M. Wolf, pp 169-176, ASM, Metals Park, OH, 1984.
11. W. B. Jones, "Ferritic Steels for High Temperature Applications," A. K. Khare, Ed., ASM, Metals Park, OH, 1983.
12. R. Page, J. R. Weertman and M. Roth, Acta metall. 30 (1982) 1357.
13. M. S. Yang, J. R. Weertman and M. Roth, Scripta metall. 18 (1984) 543.
14. M. S. Yang, J. R. Weertman and M. Roth, "Creep and Fracture of Engineering Materials and Structures", edited by B. Wilshire and D. R. J. Owen, pp 149-156, Pineridge Press, Swansea, UK, 1984.
15. M. S. Yang, J. R. Weertman and M. Roth, Fifth Risø International Symposium on Metallurgy and Materials Science, edited by N. H. Hansen, M. Eldrup, N. Hansen, D. J. Jensen, T. Leffers, H. Lilholt, O. B. Pedersen and B. N. Singh, p 589, Roskilde, Denmark, 1984.
16. M. Verrilli, S. Spooner and J. R. Weertman, to be published.
17. R. A. Page and J. Lankford, J. Am. Cer. Soc. 66 (1983) C-146.
18. R. A. Page, J. Lankford and S. Spooner, Acta metall. 32 (1984) 1275.
19. R. A. Page, J. Lankford and S. Spooner, J. Mats. Sci. 19 (1984) 3360.
20. M. J. Schmank and A. D. Krawitz, Met. Trans. A 13A (1982) 1069.
21. H. J. Prask and C. S. Choi, J. Nuclear Mats. 126 (1984) 124.
22. A. D. Krawitz, E. F. Drake, R. L. DeGroot, C. H. Vasel and W. B. Yelon, "Neutron Diffraction Studies of Cemented Carbide Composites,: Science of Hard Materials, Plenum Press, New York, p 973, 1983.
23. A. D. Krawitz, R. Roberts and J. Faber, "Residual Stress Relaxation in Cemented Carbide Composites", Second International Conference on the Science of Hard Materials, Rhodes, Greece, Sept. 23-29, 1984.
24. D. Juul Jensen, N. Hansen, J. K. Kjems and T. Leffers, Fifth Risø International Symposium on Metallurgy and Materials Science, edited by N. H. Hansen, M. Eldrup, N. Hansen, D. J. Jensen, T. Leffers, H. Lilholt, O. B. Pedersen and B. N. Singh, p 325, Roskilde, Denmark, 1984.
25. N. Berk and K. Hardman-Rhyne, to be published.
26. K. Hardman-Rhyne and N. Berk, to be published.
27. C. J. Glinka and C. H. Lochmuller, to be published.
28. G. Allen and S. E. B. Petrie, "The Physical Structure of the Amorphous State,", G. Allen and S. E. B. Petrie, Eds., Marcel Dekker, 1976.
29. C. R. Bartels, W. W. Graessley and B. Crist, J. Polymer Sci.: Polymer Letters Edn. 21 (1983) 495.
30. C. R. Bartels, B. Crist and W. W. Graessley, Macromolecules 17 (1984) 2702.
31. J. C. LaSalle, S. Spooner and L. H. Schwartz, Mats. Res. Soc. Symp. Proc. 21 (1984) 549.
32. S. P. Singhal, H. Herman and G. Kostorz, J. Appl. Cryst. 11 (1978) 572.
33. A. Salva-Ghilarducci, J. P. Simon, P Guyot and I. Ansara, Acta metall. 31 (1983) 1705.
34. M. Fatemi, C. S. Pande and H. R. Child, Phil. Mag. A 48 (1983) 479.
35. M. Fatemi, Phil. Mag., in press.